Int. J. Heat Mass Transfer. Vol. 36, No. 3, pp. 725–733, 1993
Printed in Great Britain

0017-9310/93 $6.00 + 0.00

Periodic melting within a square enclosure with an oscillatory surface temperature

C. J. HO† and C. H. CHU
Department of Mechanical Engineering, National Cheng Kung University, Tainan, Taiwan 701, R.O.C.

(*Received* 16 *December* 1991 *and in final form* 14 *February* 1992)

Abstract—This paper presents a numerical study dealing with the natural convection-dominated melting process of a pure metal (tin) from a hot vertical wall, having a uniform surface temperature with a time-dependent sinusoidally varying perturbation, of a square enclosure. The enthalpy method is adopted to model the latent heat absorption/release at the moving solid–liquid interface and the Boussinesq approximation is adhered to to simulate the natural convection flow in the melt region. Parametric simulations via a finite difference method have been directed towards the response of the melting process in the enclosure to the imposed oscillatory wall temperature. The ranges of the relevant parameters covered in the present study are $Ra = 10^3$–5×10^5, $Ste = 0.007$ and 0.07, $Sc = 0.2$–0.5, $p = 0.5$–8, and $A = 0$–0.69. Results clearly demonstrate that a steady periodic melting regime arises following a period of transient oscillatory melting. The heat transfer rates at the vertical hot and cold walls as well as the melting rate exhibit a regular temporal oscillation at a frequency equal to that of the imposed wall temperature perturbation but with phase difference. The effects of relevant parameters on the oscillatory melting behavior are investigated.

INTRODUCTION

THIS PAPER presents a numerical study of the melting process in a square enclosure due to temporally periodic heating on a vertical wall, as depicted in Fig. 1. The physical configuration considered is of fundamental interest in connection with the problem concerning a thermal management device utilizing a solid–liquid phase change material (PCM thermal management device). The periodic variation of the hot wall temperature with time simulates the boundary condition encountered in the surroundings of many thermal systems, such as cyclic solar flux and time-dependent surface temperature in electronic devices due to periodically switching the current on and off in the electronic components.

The heat transfer problem of melting from a vertical hot wall in a rectangular enclosure has received considerable research attention due to its fundamental importance in current technological applications. Comprehensive reviews of the literature concerning this problem are available [1–3]. It has been demonstrated that natural convection in the melt region can play a major role in the melting heat transfer process. Representative works on the natural-convection-dominated melting process in vertical rectangular enclosures are chronically listed in refs. [4–8]. The thermal boundary condition of the hot vertical wall considered in these previous studies is limited to that of static isothermal temperature or fixed heat flux. In many practical operations, however, the PCM inside the enclosure could be subjected to a temporally periodic thermal boundary condition, and as a result a periodic melting/solidification phenomenon arises. Several studies in the existing literature are found to deal with the periodic solid–liquid phase change heat transfer in a latent heat storage device of various geometry. Bransier [9] analyzed the conduction-dominated thermal behavior of a PCM in contact with a fluid undergoing a sinusoidal variation of temperature with time. Bransier and co-workers [10] further presented an experimental study as well as a one-dimensional modeling of periodic latent heat storage in an enclosed PCM slab. The effects of natural convection in the melt were also taken into account in the model. A finite difference analysis has been performed for the periodic thermal performance of a latent heat storage cylinder [11]. Kalhori and Ramadhyani [12] studied experimentally the heat transfer and temperature dis-

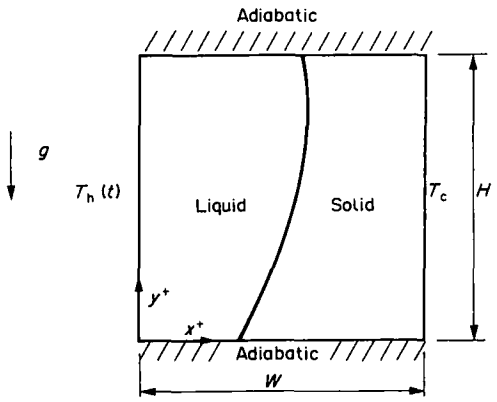

FIG. 1. Schematic description of the physical configuration.

† Author to whom all correspondence should be addressed.

NOMENCLATURE

a	amplitude of oscillatory surface temperature
A	dimensionless amplitude of oscillatory surface enthalpy, $c_{p,l}a/(\bar{\lambda}_h^+ - \lambda_c^+)$
$A_{q,c}$	oscillatory amplitude of Q_c
$A_{q,h}$	oscillatory amplitude of Q_h
A_v	oscillatory amplitude of V^*
AR	aspect ratio, W/H
c_p	specific heat
f^+	frequency
f	dimensionless frequency, f^+H^2/α_l
f_l	local liquid fraction
F_l	dimensionless local liquid fraction, f_l/L
Fo	Fourier number, $\alpha_l t/H^2$
g	gravitational acceleration
H	height of enclosure
k	thermal conductivity
L	latent heat
p	dimensionless time period, $1/f$
Pr	Prandtl number, ν_l/α_l
$\bar{q}$	average heat flux at vertical wall
Q	dimensionless heat transfer rate
Ra	Rayleigh number, $g\beta(\bar{\lambda}_h^+ - \lambda_c^+)H^3/(c_{p,l}\alpha_l\nu_l)$
Sc	subcooling factor, $(\lambda_f^+ - \lambda_c^+)/(\bar{\lambda}_h^+ - \lambda_c^+)$
Ste	Stefan number, $(\bar{\lambda}_h^+ - \lambda_f^+)/L$
t	time
T	temperature
V_m	volume of liquid PCM
V_0	total volume of PCM
V^*	volumetric fraction of liquid PCM, V_m/V_0
W	width of enclosure
x^+, y^+	Cartesian coordinates
x, y	dimensionless coordinates, x^+/H, y^+/H.

Greek symbols

α	thermal diffusivity
β	thermal volumetric expansion coefficient
λ^+	enthalpy
λ	dimensionless enthalpy, $(\lambda^+ - \lambda_c^+)/(\bar{\lambda}_h^+ - \lambda_c^+)$
ν	kinematic viscosity
ξ	dummy variable
ρ	density
ψ^+	stream function
ψ	dimensionless stream function, ψ^+/α_l
ω^+	vorticity
ω	dimensionless vorticity, ω^+H^2/α_l.

Subscripts

c	cold surface
h	hot surface
i,j	grid index
l	liquid phase
s	solid phase.

Superscripts

*	ratio of quantity for solid to that for liquid phase
$\bar{}$	average value.

tributions in a vertical annular latent heat storage unit undergoing a periodic steady state operation at which the energy recovered during solidification is equal to that stored during the melting process. Moreover, Jariwala *et al.* [13] evaluated experimentally the periodic steady state thermal performance of a vertical cylindrical latent heat storage unit containing a submerged helical coil. Also, a simple model involving the concept of a controlling process was proposed. To date, it appears that there has been no study treating detailed heat and fluid flows of natural-convection-dominated melting in a vertical enclosure subjected to a temporally periodic thermal boundary condition as considered in the present study.

In the absence of a solid–liquid phase change, the response of a natural convection flow field and heat transfer characteristics to a time-wise periodic wall temperature has recently been studied analytically and numerically [14]. A follow-up work of ref. [14] was further conducted via numerical experiments to determine the demarcation between the linear and nonlinear responses of temperature and flow fields of natural convection in an air-filled square enclosure to wall temperature oscillation of small amplitude [15]. It was found that the critical amplitude corresponding to the demarcation is a strong inverse function of the Rayleigh number. More recently, the effects of amplitude and frequency of oscillatory wall temperature on a water-filled square enclosure were investigated numerically for a fixed Rayleigh number [16].

The study to be described here appears to be the first effort to explore the response of a natural-convection-dominated melting process in an enclosure to a time-dependent periodic variation of temperature at the vertical hot wall. More specifically, the effects of the oscillatory variation of wall temperature on the flow field and heat transfer associated with the melting process in a square enclosure are investigated by means of numerical simulations of the problem.

MATHEMATICAL FORMULATION

As depicted schematically in Fig. 1, two-dimensional melting of a solid PCM in a vertical rectangular enclosure is modeled mathematically. The solid PCM is assumed to be initially subcooled at a uniform tem-

perature T_c. At time $t = 0$, the left-hand vertical wall is isothermally heated with a sinusoidal perturbation about a mean hot wall temperature $\bar{T}_h$, with amplitude a and frequency f^+. The time-dependent hot wall temperature remains above the fusion temperature of the PCM at all times. The right-hand vertical wall is kept isothermal at T_c, and the horizontal walls of the enclosure are assumed adiabatic. To facilitate the formulation, the following further assumptions are adopted:

(1) The thermophysical properties of the PCM are independent of temperature.

(2) The fluid flow in the melt region is laminar and two-dimensional.

(3) The Boussinesq approximation is valid.

(4) The viscous dissipation and volume change due to the solid–liquid phase change are negligible.

With the foregoing, the normalized governing partial differential equations for the problem under consideration are formulated in terms of stream function, vorticity, and enthalpy similar to those used in ref. [17]:

$$\frac{\partial \omega}{\partial Fo} + u\frac{\partial \omega}{\partial x} + v\frac{\partial \omega}{\partial y} = Pr\left(\frac{\partial^2 \omega}{\partial x^2} + \frac{\partial^2 \omega}{\partial y^2}\right) + Pr\,Ra\frac{\partial \lambda}{\partial x} \tag{1}$$

$$\frac{\partial^2 \psi}{\partial x^2} + \frac{\partial^2 \psi}{\partial y^2} = -\omega \tag{2}$$

$$\frac{\partial \lambda}{\partial Fo} + u\frac{\partial \lambda}{\partial x} + v\frac{\partial \lambda}{\partial y} = \alpha^*\left(\frac{\partial^2 \lambda}{\partial x^2} + \frac{\partial^2 \lambda}{\partial y^2}\right) - \frac{(1-Sc)}{Ste}\frac{\partial F_l}{\partial Fo}. \tag{3}$$

Here the energy equation, equation (3), is applied to the entire PCM including the solid–liquid interface, while the vorticity and the stream function equations, equations (1) and (2), are solved only for the melt region of the PCM. Moreover, the dimensionless thermal diffusivity ratio α^* in equation (3) is determined based on the liquid fraction in the control volume about a grid point as

$$\alpha^* = F_l + (1-F_l)\frac{\alpha_s}{\alpha_l}. \tag{4}$$

The initial and boundary conditions for the problem can be written as:

at $Fo = 0$,

$$\psi = \omega = \lambda = 0 \tag{5}$$

for $Fo > 0$,

$y = 0$ or $1, 0 \leqslant x \leqslant AR$;

$$\psi = \frac{\partial \lambda}{\partial y} = 0 \tag{6a}$$

$x = 0, 0 \leqslant y \leqslant 1$;

$$\psi = 0, \lambda = 1 + A\sin(2\pi\, Fo/p) \tag{6b}$$

$x = AR, 0 \leqslant y \leqslant 1$;

$$\psi = 0, \lambda = 0 \tag{6c}$$

at the solid–liquid interface;

$$\psi = 0, \lambda = Sc. \tag{6d}$$

Furthermore, the heat transfer rate through the hot and cold walls of the enclosure is, respectively, presented by means of dimensionless heat transfer rates defined as

$$Q_h = -\frac{k^*}{c^*}\int_0^1 \left(\frac{\partial \lambda}{\partial x}\right)_{x=0} dy = \frac{c_{p,l} H \bar{q}_h}{k_l(\bar{\lambda}_h^+ - \lambda_c^+)} \tag{7a}$$

$$Q_c = -\frac{k^*}{c^*}\int_0^1 \left(\frac{\partial \lambda}{\partial x}\right)_{x=AR} dy = \frac{c_{p,l} H \bar{q}_c}{k_l(\bar{\lambda}_h^+ - \lambda_c^+)}. \tag{7b}$$

METHOD OF SOLUTION

The set of governing differential equations, equations (1)–(3), subjected to the initial/boundary conditions, equations (5) and (6), was solved numerically by means of a finite difference method. The differential equations were discretized by using second-order central differencing for the spatial derivatives except the convective terms, for which the second upwind scheme [18] was adopted. The time derivatives were approximated by a forward difference. The resulting finite difference equations at each time step were solved iteratively by using a line relaxation scheme. The solution procedure used in the present study is essentially the same as that described in refs. [17, 19] and need not be repeated here. The convergence criteria adopted for each field variable ($\xi = \psi, \omega, \lambda$) in the iteration procedure at each time step is

$$\frac{|\xi_{i,j}^{n+1} - \xi_{i,j}^{n}|_{\max}}{|\xi_{i,j}^{n+1}|_{\max}} \leqslant 10^{-4}, \tag{8}$$

where the superscript n denotes the iteration level.

A 41×41 uniform mesh system was adopted for the simulation as a result of a series of test calculations for the grid dependency. For instance, the results of the heat transfer rate as well as the melted fraction of PCM for $Ra = 5 \times 10^5$, $Pr = 0.0157$ (tin), $Ste = 0.007$, $A = 0.69$, $p = 8$ using a mesh of 41×41 differ from those using the 51×51 mesh within 1%. Furthermore, the time step selected for the simulation depends on the period of the oscillatory wall temperature; one period of the wall temperature oscillation is subdivided into at least 400 time steps.

In order to validate the computer code developed in the present study, a preliminary calculation was conducted for the limiting case of natural-convection-dominated melting of pure tin from a time-independent isothermal vertical wall in a shallow rectangular enclosure ($H/W = 0.75$) like that investigated in refs. [20, 21]. Comparison of the present calculation for the melting front profiles at different times with their data is shown in Fig. 2. It is evident from the figure that our simulation yields results somewhat closer to the experimental data of ref. [20]

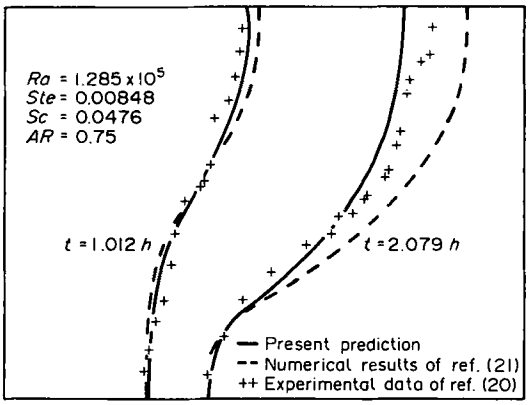

FIG. 2. Comparison of the predicted melting fronts of pure tin in a shallow rectangular enclosure with the existing data.

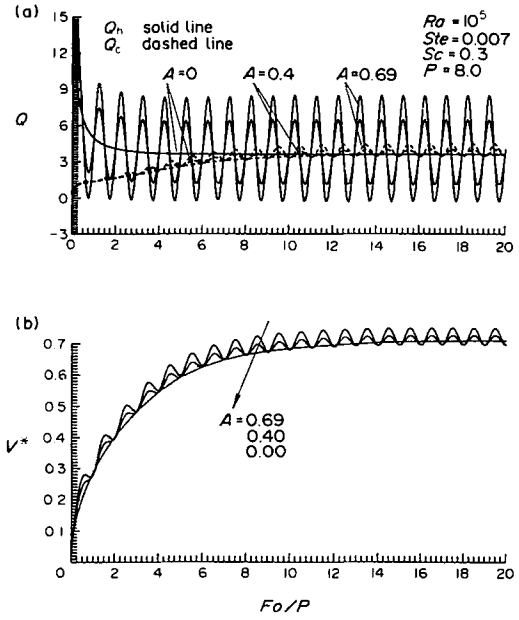

FIG. 3. Temporal variations of the heat transfer rates at the vertical walls (a) and the melting rate (b).

than the prediction of ref. [21]. This may be in part due to the fact that the numerical prediction of ref. [21] did not take into account the subcooling of PCM that existed in the experiment [20].

RESULTS AND DISCUSSION

From the foregoing formulation, the melting process considered in the present study is governed by the following parameters: the Rayleigh number Ra, the Prandtl number Pr, the Stefan number Ste, the subcooling factor Sc, the dimensionless time period p (or the frequency f), the dimensionless amplitude A, and the aspect ratio AR. Numerical simulations have been performed for pure tin as the PCM with the relevant parameters in the following ranges: $Pr = 0.0157$, $Ra = 10^3$–5×10^5, $Ste = 0.007$ and 0.07, $Sc = 0.2$–0.50, $p = 0.5$–8.0 ($f = 0.0625$–2), $A = 0$–0.69, and $AR = 1$. The thermophysical properties of pure tin are available in refs. [20, 21]. All calculations were conducted on a personal computer PC-AT486 that requires more than 29 h for a typical simulation. Due to the long computational time required for the simulation, calculations for extensive combinations of these parameters have not been possible. A total of 20 numerical simulations have been performed. Presentation of the simulation results will be mainly focused on the influences of the parameters Ste, A, p, Ra, and Sc on the heat transfer characteristics and the melting rate in the enclosure under time-dependent wall temperature perturbation.

Unlike the better known melting behavior in a vertical enclosure with static thermal boundary conditions, it is expected that the melting process will proceed somewhat differently with an oscillatory perturbation of temperature with time on the vertical hot wall. In general, there are two distinct regimes that emerge as the melting process proceeds in the presence of an oscillatory wall temperature. Following an initial transient oscillatory regime, a steady periodic melting regime arises, as exemplified in Fig. 3 for $Ra = 10^5$, $Ste = 0.007$, $Sc = 0.3$, and $p = 8$ ($f = 0.125$) with different amplitudes. The time-wise variations of the heat transfer rates through the vertical walls and the melted volume fraction are presented in Fig. 3. An overview of the figure clearly reveals that the heat transfer rates as well as the melting rate reach a steady periodic variation with time following different periods of the initial transient oscillatory regime, respectively. Specifically, the heat transfer rate through the hot wall, Q_h, starts to exhibit transient oscillatory variation after action of the first half cycle of the oscillatory wall temperature, as shown in Fig. 3(a). Starting from the fourth cycle of the wall temperature oscillation, the regime of the steady periodic variation of Q_h appears. Furthermore, it can be noticed from the figure that the oscillation of Q_h is in phase with the oscillatory wall temperature at the same frequency.

On the other hand, the initial transient regime of the heat transfer rate through the cold wall, Q_c, as also displayed in Fig. 3(a), features transient oscillatory variation with gradually higher local maxima in accordance with the oscillatory action of the hot wall temperature. The gradual increase of the local maximum of Q_c during the initial transient regime also reflects the dependence of the degree of penetration of the wall temperature oscillation upon the melting front position, namely the melted fraction V^*. With the oscillatorily increasing melted fraction as depicted in Fig. 3(b), the heat transfer rate at the static isothermal cold wall gradually becomes stimulated. After the seventeenth cycle on the hot wall temperature oscillation, the value of Q_c reaches a steady periodic regime, having the same frequency as that of the imposed hot wall temperature perturbation but with phase difference. Moreover, the amplitude of Q_c

oscillation appears to be much smaller than that for Q_h, reflecting the damping effects due to the solid–liquid phase change process on the penetration of the hot wall temperature perturbation.

As for the melting rate, a steady periodic regime occurs after the sixteenth cycle on the imposed wall temperature oscillation, as shown in Fig. 3(b). The oscillatory variation of the melted fraction implies cyclic occurrence of re-solidification at the solid–liquid interface in response to the oscillatory heat inflow and outflow through the vertical walls. Another interesting fact that can be observed from the figure is that the periodic variation of Q_c is somewhat in phase with that of the melting rate. Furthermore, the oscillation amplitude of the heat transfer rate Q_h as well as the local maximum values of Q_c and V^* tend to increase with the increase of the imposed oscillation amplitude at the hot wall, while the local minimum values of Q_c and V^* appear to be rather insensitive to the variation of the imposed oscillation amplitude.

As the Stefan number is increased, the occurrence of the steady periodic melting behavior becomes greatly promoted, as illustrated in Fig. 4 for $Ste = 0.07$. The heat transfer rates through the vertical walls, Q_h and Q_c, display the steady periodic variation soon after the first oscillation cycle of the hot wall temperature, indicating greatly enhanced penetration of the wall temperature perturbation on the melting behavior in the enclosure. The sequence of contour maps for streamline and enthalpy distributions at nine instants spanned over the fifth cycle of the hot wall temperature oscillation as denoted in Fig. 4(a) is displayed in Fig. 5. The dashed lines in the contour plots indicate

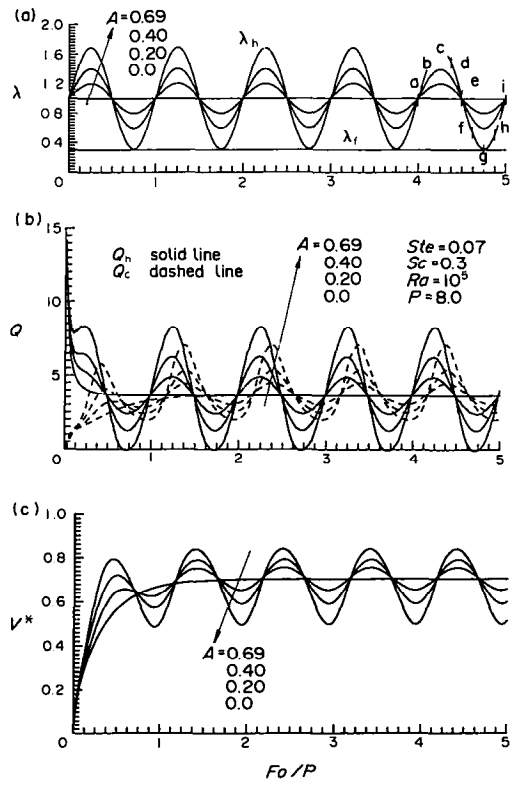

FIG. 4. Temporal variations of the imposed enthalpy oscillation at the hot wall (a), the heat transfer rates (b) and the melting rate (c).

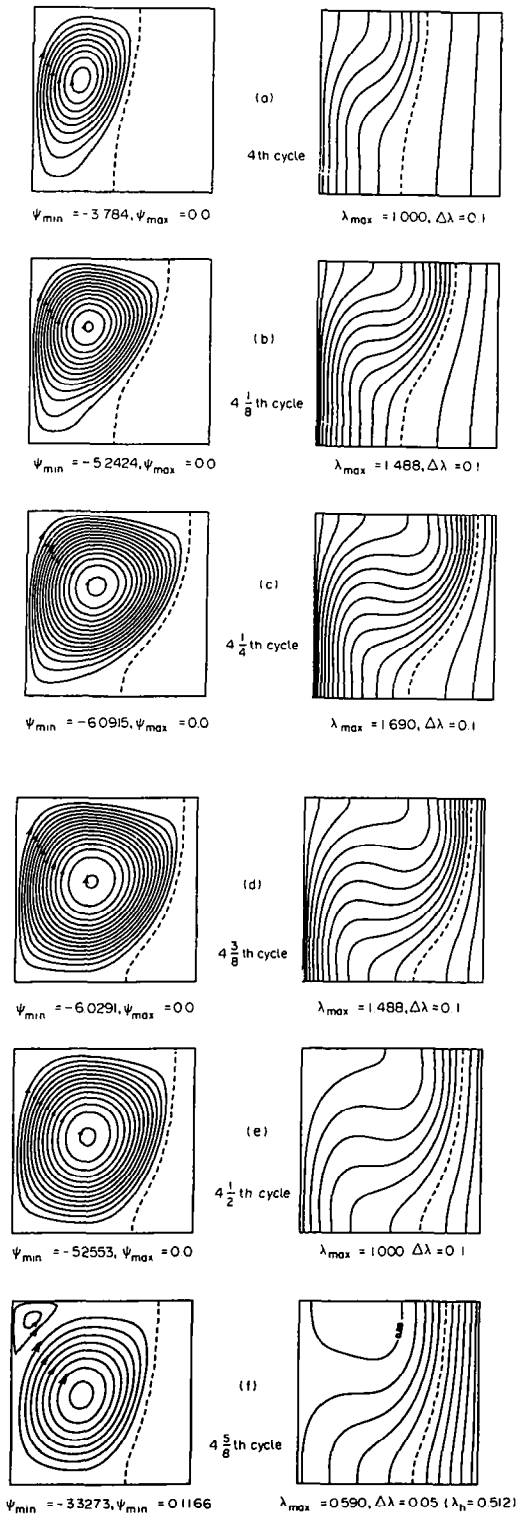

FIG. 5. Periodic streamline (left) and iso-enthalpy contour (right) plots at different instants denoted in Fig. 4(a).

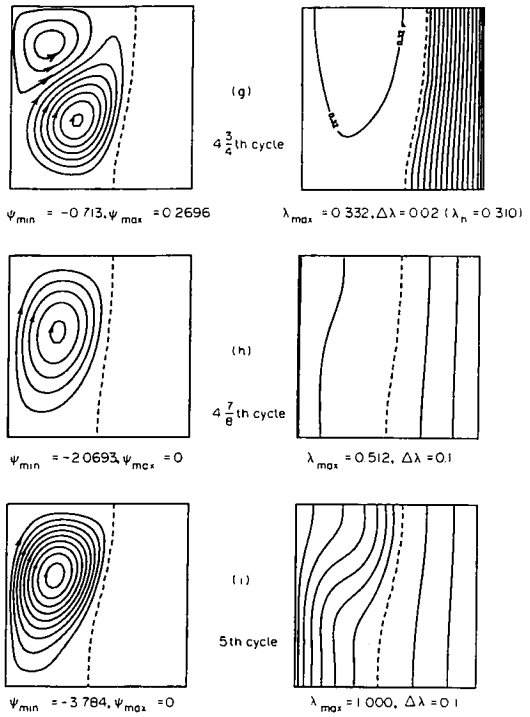

FIG. 5 (*continued*).

the locations of the melting front. During the first quarter of the cycle, the unicellular flow field in the melt region continues to intensify with the hot wall temperature rising to its maximum; the enthalpy gradient at the hot wall, and thus the heat transfer rate Q_h, reach their maximum accordingly. With the subsequent fall of the hot wall temperature through the second and third quarters of the cycle, the clockwise circulation in the melt is seen to be progressively impeded, and a counter-rotating secondary eddy is detected growing at the upper left corner region, as shown in Figs. 5(f) and (g). Meanwhile, as seen from these plots, the thermal boundary layer on the hot wall becomes loose with the declining hot wall temperature and a warm pocket of melt at temperature higher than the hot wall is detected to float in the top region of the melt zone. In particular, at the end of the third quarter of the cycle, an essentially isothermal melt slightly warmer than the hot wall is observed and a minute back heat flow arises at the hot wall, as witnessed by the slight negative value of Q_h in Fig. 4(b) at the corresponding time. Resemblance to the above-described back heat flow phenomenon was also found for the pure natural convection of water in a square enclosure without a solid–liquid phase change [16]. Moreover, under the extraction of the sensible heat from the solid PCM through the cold wall, a re-solidification phenomenon occurs and hence the movement of the solid–liquid interface is reversed starting from the second quarter, as witnessed in Figs. 5(d)–(i). This re-solidification process is seen to continue through the fourth quarter of the cycle and, at the same time, the flow structure as well as the enthalpy distribution in the melt region during this time interval evolve back to those observed at the beginning of the cycle.

Figure 6 is intended to demonstrate the effect of the time period of the wall temperature oscillation on the periodic melting behavior for $Ste = 0.07$, $Sc = 0.3$, $Ra = 10^5$, and $A = 0.4$. It is evident from the curves for the heat transfer rates shown in Fig. 6(a) that the shorter time period, namely higher oscillation frequency, tends to advance and strengthen the steady periodic heat transfer behavior at both vertical walls but leads to weaker thermal penetration, as indicated by the smaller oscillation amplitudes of the heat transfer rate through the cold wall as well as of the melting rate variation illustrated in Fig. 6(b).

The influence of the Rayleigh number is conveyed in Fig. 7 for $Ste = 0.07$, $Sc = 0.3$, $p = 8$, and $A = 0.4$. The amplitudes of the heat transfer rates at both vertical walls exhibit strong dependence on the Rayleigh number; the increase of the Rayleigh number greatly amplifies the oscillation amplitudes of Q_h and Q_c. Yet, the amplitude of the oscillatory melting rate, Fig. 7(b), displays little dependence on the Rayleigh number. Furthermore, Fig. 7 reveals that the increase of Ra results in a significant increase of the mean values of the heat transfer rates and the melting rate in the steady periodic melting regime. This further reflects the dominant role played by natural convection during the melting process in the presence of temporal wall temperature perturbation.

Next, the variation of the subcooling factor Sc is considered as presented in Fig. 8. The heat transfer rate at the hot wall is, as expected, markedly enhanced with a slightly larger oscillation amplitude for the

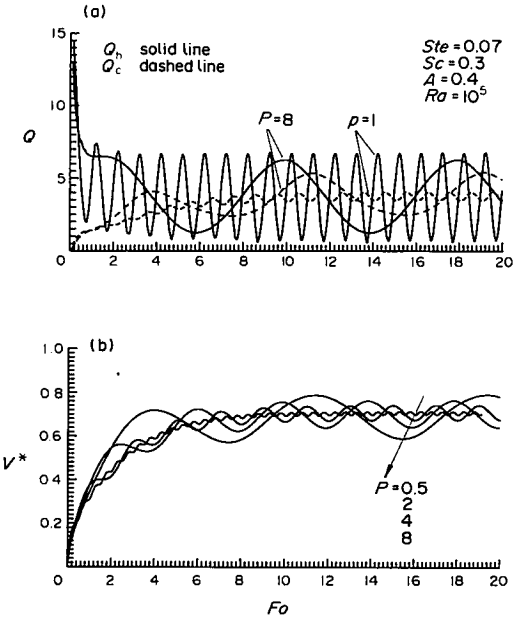

FIG. 6. Influence of the time period on the heat transfer rates and the melting rate.

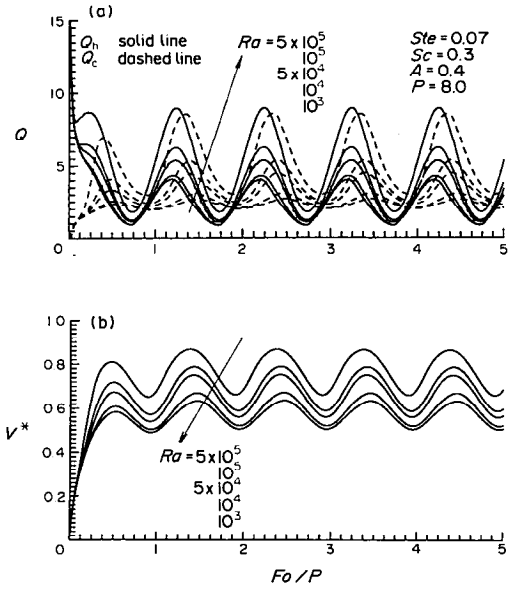

FIG. 7. Effect of the Rayleigh number on the heat transfer rates and the melting rate.

lower subcooling factor, as depicted in Fig. 8(a). As for the heat transfer rate at the cold wall, a somewhat different evolution occurs. During the initial first cycle of the heating action, the higher subcooling factor leads to a lower melting rate, as shown in Fig. 8(b), because the higher subcooled solid PCM drains more energy rapidly from the solid–liquid interface by conduction. Consequently, the conduction heat transfer rate through the cold wall is markedly higher with the higher subcooling factor. As the melt region enlarges with time, the thermal gradient in the solid PCM increases accordingly. The higher melting rate due to the lower subcooling factor then yields a higher increasing rate of the temperature gradient in the solid, and hence of the heat transfer rate Q_c, than the case of the higher Sc. The value of Q_c for the lower Sc gradually catches up and eventually surpasses that for the higher Sc such that the lower subcooling factor induces stronger oscillatory heat transfer through the cold wall. Moreover, the occurrence of the above-described reversal of the influence of the subcooling factor on Q_c is found to be greatly delayed until the fifth cycle of the heating action with the smaller Stefan number, $Ste = 0.007$ (not shown here). Further inspection of Fig. 8(b) reveals that the oscillation amplitude of the melting rate intensifies noticeably with the increasing subcooling factor.

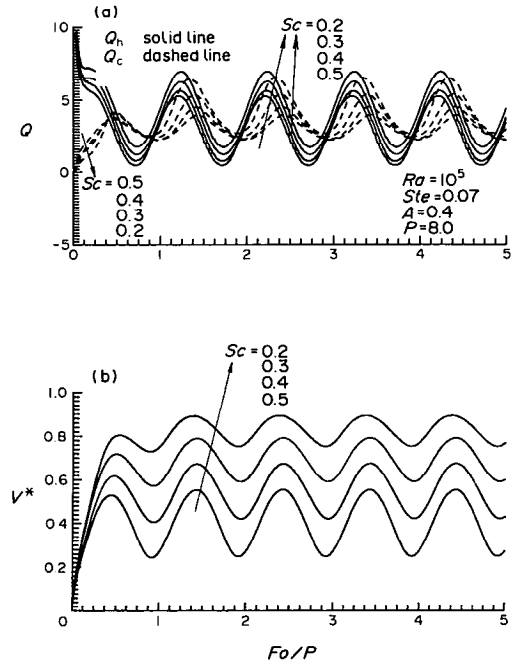

FIG. 8. Dependence of temporal variation of the heat transfer rates and the melting rate on the subcooling factor.

To further quantify the heat transfer results and the melting rate during the steady periodic melting regime, the periodic mean values as well as the oscillation amplitudes of the heat transfer rates at both vertical walls and the melting rate are plotted versus the relevant parameters in Fig. 9. It should be noted that the periodic mean values at both vertical walls under the steady periodic operation are expected to be balanced, and the results from our simulations show that the heat balance is always within 2%, so that only the curves for the hot wall are drawn in the figure. An overview of Figs. 9(a) and (b) indicates that the periodic mean values of both the heat transfer rate and the melting rate show little dependence on either the time period or the amplitude of the imposed wall temperature perturbation. That is, the periodic mean heat transfer rate as well as the mean melting rate in the enclosure subjected to an oscillatory wall temperature perturbation is approximately equal to that with a static wall temperature at the mean value of the perturbation. This finding is also similar to that obtained in ref. [16] for pure natural convection in the enclosure. On the other hand, as expected, the periodic mean values of the heat transfer rate and the melting rate are strongly affected by the subcooling factor as well as the Rayleigh number. The increase of the subcooling factor gives rise to a drastic decrease of the heat transfer rate and the melting rate, as shown in Fig. 9(c). Figure 9(d) shows that the higher Rayleigh number leads to an enhanced mean heat transfer rate and a higher melting rate.

Moreover, the oscillation amplitudes for the heat transfer rates and the melting rate displayed in Fig. 9 are scaled by the amplitude of the imposed wall temperature perturbation. From Fig. 9(a), the longer time period of the imposed wall temperature perturbation results in larger amplitudes of both the heat transfer rates at the cold wall and the melting rate, while the opposite occurs for the amplitude of the heat transfer at the hot wall, which decreases significantly with the time period increasing up to 4 and thereafter remains rather unchanged, indicative of a quasi-linear

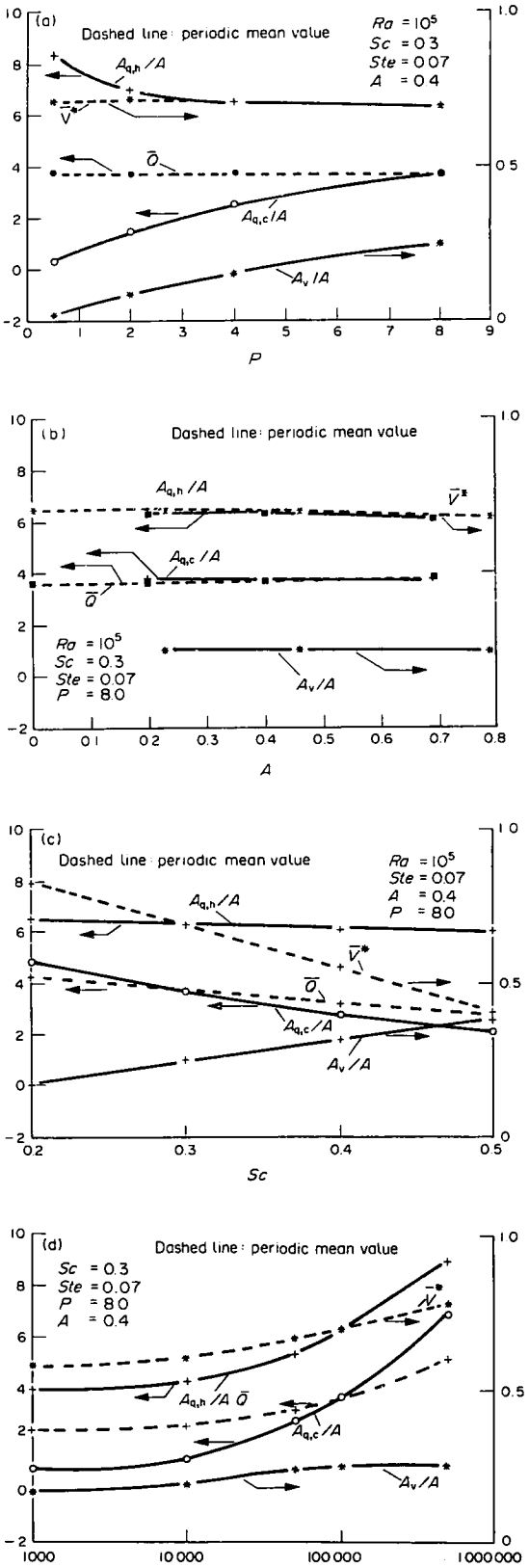

FIG. 9. Effects of the relevant parameters on the periodic mean values and the oscillation amplitudes of the heat transfer rates and the melting rate during the steady periodic melting regime.

period response behavior. Also, the variation of the imposed amplitude of the wall temperature oscillation is found to yield a quasi-linear effect on the amplitudes of the heat transfer rates, Q_h and Q_c, as well as the melting rate, as revealed by the nearly horizontal straight lines of the scaled amplitudes shown in Fig. 9(b). Next, in Fig. 9(c), in conformity with that depicted in Fig. 8(a), the amplitudes of Q_h and Q_c reduce linearly with the increase of the subcooling factor, while the amplitude of V^* shows a linear increase with increasing subcooling factor. Moreover, the increasing Rayleigh number amplifies drastically the oscillation amplitudes of both Q_h and Q_c as illustrated in Fig. 9(d). Yet, the melting rate appears to exhibit a somewhat moderate dependence on the Rayleigh number.

Finally, by means of least-square regression, the following correlations have been developed for the results of the periodic mean values as well as the oscillation amplitudes of the heat transfer rates at the vertical walls and the melting rate during the steady periodic melting regime for $Ste = 0.07$, $Sc = 0.2$–0.5, and $A = 0$–0.69:

$$\bar{V}^* = 0.641(1-1.27Sc)Ra^{0.053}p^{-0.016}(1-0.058A) \tag{9a}$$

for $Ra = 10^4$–5×10^5 and $p = 0.5$–8, with average deviation = 0.81%

$$\bar{Q} = 0.563(1-0.919Sc)Ra^{0.189}p^{0.004}(1+0.088A) \tag{9b}$$

for $Ra = 10^4$–5×10^5 and $p = 0.5$–8, with average deviation = 2.1%

and

$$A_v = 0.007A(1+19.4Sc)\left(\frac{Ra^{0.293}}{1+Ra^{0.237}}\right)\left(\frac{p^{1.40}}{1+p^{0.842}}\right) \tag{10a}$$

for $Ra = 10^3$–5×10^5 and $p = 0.5$–8, with average deviation = 2.9%

$$A_{q,h} = 0.871A(1-0.240Sc)Ra^{0.196}p^{-0.097} \tag{10b}$$

for $Ra = 10^4$–5×10^5 and $p = 0.5$–8, with average deviation = 2.3%

$$A_{q,c} = 0.019A(1-1.35Sc)Ra^{0.426}\left(\frac{p^{1.63}}{1+p^{1.16}}\right) \tag{10c}$$

for $Ra = 10^4$–5×10^5 and $p = 1$–8, with average deviation = 3.7%.

CONCLUDING REMARKS

Natural-convection-dominated melting of pure tin in a vertical square enclosure with a temporally oscillatory hot wall temperature is studied numerically. A

steady periodic melting regime arises following an initial transient oscillatory melting stage. During the steady periodic melting regime, the heat transfer rates as well as the melting rate exhibit steady oscillation with frequency equal to that of the imposed wall temperature perturbation but with phase difference. For the ranges of parameters considered in the present simulation, the results clearly demonstrate that the occurrence of the steady periodic melting regime is greatly advanced with increasing Stefan number. The steady oscillatory heat transfer characteristics at both vertical walls are found to be similar to those reported for the pure natural convection in an enclosure without the solid–liquid phase change. The steady oscillation of the heat transfer rate at the hot wall is in phase with the hot wall temperature perturbation, while the heat transfer through the cold wall oscillates in phase with the melting rate. The periodic mean values of the heat transfer rates as well as the melting rate are strongly affected by the Rayleigh number and the subcooling factor, but are rather insensitive to the oscillation amplitude or the time period of the imposed wall temperature perturbation. Moreover, the oscillation components of the heat transfer rates as well as the melting rate respond differently to the variation of amplitude and period of the imposed wall temperature perturbation, the Rayleigh number, the subcooling factor, and the Stefan number. In particular, the oscillation amplitudes of the heat transfer rate and the melting rate exhibit a quasi-linear response to the variation of the imposed amplitude and the subcooling factor.

The numerical simulations undertaken in the present study are certainly far from complete; further work for more extensive investigation for wider ranges of the relevant parameters of the problem is needed as well as the experimental verification of the numerical predictions.

REFERENCES

1. R. Viskanta, Phase-change heat transfer. In *Solar Heat and Storage: Latent Heat Materials* (Edited by G. A. Lane), pp. 153–222. CRC Press, Boca Raton, Florida (1983).
2. R. Viskanta, Natural convection in melting and solidification. In *Natural Convection: Fundamentals and Applications* (Edited by S. Kakac *et al.*), pp. 845–877. Hemisphere, Washington, DC (1985).
3. R. Viskanta, Heat transfer during melting and solidification of metals, *J. Heat Transfer* **110,** 1205–1219 (1988).
4. N. W. Hale, Jr. and R. Viskanta, Photographic observation of the solid–liquid interface motion during melting of a solid heated from an isothermal vertical wall, *Lett. Heat Mass Transfer* **5,** 329–337 (1978).
5. C. J. Ho and R. Viskanta, Heat transfer during melting from an isothermal vertical wall, *J. Heat Transfer* **106,** 12–19 (1984).
6. M. Okada, Analysis of heat transfer during melting from a vertical wall, *Int. J. Heat Mass Transfer* **27,** 2057–2066 (1984).
7. C. Bénard, D. Gobin and F. Martinez, Melting in rectangular enclosures: experiments and numerical simulations, *J. Heat Transfer* **107,** 794–803 (1985).
8. Z. Zhang and A. Bejan, Melting in an enclosure heated at constant rate, *Int. J. Heat Mass Transfer* **32,** 1063–1076 (1989).
9. J. Bransier, Stockage periodique par chaleur latente aspects fondamentaux liés a la cinétique des transferts, *Int. J. Heat Mass Transfer* **22,** 875–883 (1979).
10. D. Delaunay, J. Bransier and J. P. Bardon, Experimental study and numerical model for a phase-change thermal energy storage unit. In *Heat Transfer*—1982, Vol. 6, pp. 449–454. Hemisphere, Washington, DC (1982).
11. M. E. McCabe, Periodic heat conduction in energy storage cylinders with change of phase. ASME paper 86-HT-12 (1986).
12. B. Kalhori and S. Ramadhyani, Studies on heat transfer from a vertical cylinder, with or without fins, embedded in a solid phase change medium, *J. Heat Transfer* **107,** 44–51 (1985).
13. V. G. Jariwala, A. S. Mujumdar and M. E. Weber, The periodic steady state for cyclic energy storage in paraffin wax, *Can. J. Chem. Engng* **65,** 899–906 (1987).
14. H. Q. Yang, K. T. Yang and Q. Xia, Periodic laminar convection in a tall vertical cavity, *Int. J. Heat Mass Transfer* **32,** 2199–2207 (1989).
15. Q. Xia and K. T. Yang, Linear response of the temperature and flow fields in a square enclosure to imposed wall temperature oscillations. In *Heat Transfer*—1990, Vol. 3, pp. 271–276. Hemisphere, Washington, DC (1990).
16. M. Kazmierczak and Z. Chinoda, Transient natural convection in a cavity with an oscillatory surface temperature, *Third ASME/JSME Thermal Engng Proc.*, Vol. 1, pp. 121–129 (1991).
17. W. Y. Raw and S. L. Lee, Application of weighting function scheme on convection–conduction phase change problems, *Int. J. Heat Mass Transfer* **34,** 1503–1513 (1991).
18. P. J. Roache, *Computational Fluid Dynamics*. Hermosa, Albuquerque, New Mexico (1976).
19. S. L. Lee and R. Y. Tzong, An enthalpy formulation for phase change problem with a large thermal diffusivity jump across the interface, *Int. J. Heat Mass Transfer* **34,** 1491–1502 (1991).
20. R. Viskanta and F. Wolff, Melting of a pure metal from a vertical wall, *Exp. Heat Transfer* **1,** 17–30 (1987).
21. C. Bénard and D. Gobin, Numerical simulation of melting process for metals. In *Multiphase Flow, Heat and Mass Transfer*, ASME HTV-Vol. 109, pp. 55–60. ASME, New York (1989).